Forensic Engineering of Advanced Polymeric Materials. Part 1 – Degradation Studies of Polylactide Blends with Atactic Poly[(*R,S*)-3-hydroxybutyrate] in Paraffin

J. Rydz,[a,b,*] K. Wolna-Stypka,[a] G. Adamus,[a] H. Janeczek,[a] M. Musioł,[a] M. Sobota,[a] A. Marcinkowski,[a] A. Kržan,[c] and M. Kowalczuk[a,d,*]

[a]Polish Academy of Sciences, Centre of Polymer and Carbon Materials, 34 M. Curie-Skłodowska St., 41–800 Zabrze, Poland

[b]Bulgarian Academy of Sciences, Institute of Polymers, Acad. Georgi Bonchev St., Bl. 103A, 1113 Sofia, Bulgaria

[c]National Institute of Chemistry, Laboratory for Polymer Chemistry and Technology, Hajdrihova 19, 1000 Ljubljana, Slovenia

[d]University of Wolverhampton, Faculty of Science and Engineering, Department of Biology, Chemistry and Forensic Science, Wulfruna Street, Wolverhampton, WV1 1SB, UK

doi: 10.15255/CABEQ.2014.2258

Original scientific paper
Received: May 27, 2014
Accepted: June 4, 2015

The degradation of the advanced polymeric materials: blends of polylactide with poly[(*R,S*)-3-hydroxybutyrate] was studied in paraffin (an ingredient used in cosmetics) and compared with the degradation of pure poly[(*R,S*)-3-hydroxybutyrate]. The interaction between the polymeric materials studied and the paraffin was monitored during the degradation experiments, and the effects of this interaction were reported. Gel permeation chromatography, atomic force microscopy, electrospray mass spectrometry, nuclear magnetic resonance, differential scanning calorimetry and thermal gravimetric analysis revealed that degradation of the investigated materials occurs in the presence of paraffin. In the blends, poly[(*R,S*)-3-hydroxybutyrate] content was found to extend the disintegration time, and for the blends with good miscibility, reduced the degradation rate in the first step of degradation.

Key words

poly[(*R,S*)-3-hydroxybutyrate], polylactide blend, aliphatic polyesters, forensic science, (bio)degradable polymer, degradation, paraffin

Introduction

Classical forensic polymer engineering concerns a study of failure in polymer products. This area of science comprises fracture of plastic products, or any other reason why such a product fails in service, or fails to meet its specification.[1] So far, most of the reported case studies concern *ex-post* investigations of traditional polymeric materials such as PE, PP, PS, PVC, ABS or their thermoplastic composites. Little is known about forensic engineering of novel and advanced polymeric materials. Thus, there is a real gap in this area of knowledge. Furthermore, the *ex-ante* studies are needed to define and minimise the potential failure of novel polymer products before specific applications. Environmental stress cracking (ESC) is one of the most common causes of unexpected brittle failure of thermoplastic (especially amorphous) polymers. The rate of ESC is dependent on many factors, including, for example, the polymer's chemical composition, bonding, crystallinity, surface roughness, molar mass and residual stress. It also depends on the chemical nature of liquid media and the temperature of the system. Thus, evaluation and understanding of the structure, properties and behaviour of advanced polymer materials for perspective practical applications is needed, especially in the field of compostable polymer packages of long-life products, such as cosmetics or household chemicals.

Because of the slow environmental degradation of traditional packaging, the use of conventional plastics is accompanied by significant ecological problems. To reduce plastic waste from the packaging industry, biodegradable polymers have become interesting alternatives, for packages with a long shelf life.[2] The most important environmentally friendly plastics are generally based on aliphatic polyesters, such as poly(lactic acid), poly(3-hy-

* Corresponding author: Tel: (+359) 2 979 2285, Tel/Fax: (+359) 2 870 03 09, e-mail: jrydz@cmpw-pan.edu.pl, M.Kowalczuk@wlv.ac.uk

droxybutyrate), polycaprolactone or polyesteramides.[3]

Polylactide (PLA) is an attractive alternative to conventional plastics because of its excellent material properties, which enable a variety of potential applications in various areas. PLA can form a semicrystalline or a fully amorphous material, depending on its stereochemical structure and thermal history, and can exhibit crystal polymorphism.[4,5] The degradation process of polylactide in various environments has been thoroughly investigated.[6–14]

Natural poly(3-hydroxybutyrate) (PHB) has found a number of applications in food packaging, biomedical and pharmaceutical industry. However, its use is currently limited due to the high cost of production and the physical properties.[15] PHB production cost is dependent on a number of factors, such as substrate, chosen strain, cultivation strategy and downstream processing, utilisation of substrates,[15–19] modelling,[20] proper experimental design[21,22] and the development of a new recovery method.[23,24] Tacticity of poly(3-hydroxybutyrate) chain directly influences the properties of this polymer. Atactic PHB is a low glass transition (ca. 0 °C), amorphous polymer and behaves as an elastomer at room temperature. In blends, it is used to improve flexibility and impact resistance, while the isotactic one shows interesting processing properties, but it has a high melting point.[25,26]

A synthetic analogue of aliphatic biopolyester, poly[(*R*)-3-hydroxybutyrate] – poly[(*R,S*)-3-hydroxybutyrate] ((*R,S*)-PHB) – has been recognised to be a suitable modifier for (bio)degradable polymers, such as the brittle polylactide or the highly crystalline polyhydroxyalkanoates (PHA)s of bacterial origin.[27,28] The ring-opening polymerisation of β-butyrolactone with various types of catalysts leads to poly(3-hydroxybutyrate)s of different tacticities, which mimic those polymers found in nature.[29] The hydrolytic degradation products for both (*R*)- and (*S*)-3-hydroxybutyrate are nontoxic.[30,31] The hydrolysis of these polyesters produces shorter chains with acid and hydroxy terminal groups.[32] The hydrolytic degradation of synthetic and natural PHB in phosphate buffer at 70 °C was reported by Kurcok *et al*.[29] The chemical microstructure has been revealed to have no substantial influence on the mechanism for hydrolytic degradation of atactic and isotactic PHB. Atactic PHB degraded faster than the semicrystalline polymer.[28,29] The results show that PHB with a high-molar mass degrades relatively slowly at physiological pH values (7.0–7.4). Random scission of the polymer chains occurs first, followed by mass loss and further decomposition of the samples.[33] The major monomeric products from the acidic or alkaline hydrolysis of PHB were 3-hydroxybutyric acid and crotonic acid.[34,35]

Blending two polymers is a way to combine the complementary properties of the individual components. Polymer blends of components with low- or high-molar masses are used to obtain materials with controllable physical or thermal properties and degradability, and offer opportunities to obtain competitive polymer materials that maintain a specific property, such as biodegradability, compared to traditional polymers. Various attempts have been made to blend PLA or PHB with synthetic or natural polymers and to determine the influence of the components on the properties and biodegradability of the resulting material.[36–41] Blends of poly(L-lactide) (PLLA) with natural or synthetic PHB were miscible, or semi-miscible depending on composition, when one compound possessed a low molar mass, and were immiscible with high-molar mass compounds, e.g. PLLA, natural or synthetic PHB and PHBV.[37,42–46]

The degradation rate and mechanical properties are key factors in many applications, especially in packaging materials for long shelf life applications, of degradable polymers.[47] Recently, we originally demonstrated that the degradation of PLA films occurs in paraffin because of the residual water content. An autocatalytic effect was observed during the erosion of PLA film samples,[48,49] and this observation extended the previous investigation conducted by Vert.[50,51]

In blended systems, miscibility is one of the most important factors affecting the final properties of the material. PLA blends have been studied, and the effect of miscibility on the surface morphologies and the structures of the blends has been investigated;[39,52] however, the relationship between the phase structure and the degradation of PLA/(*R,S*)-PHB blends in cosmetic simulants has not yet been studied. In this contribution has been reported the degradation in paraffin at 70 °C of polylactide-based rigid films with poly[(*R,S*)-3-hydroxybutyrate] in comparison with that of the plain (*R,S*)-PHB. Analysis of the surface erosion of the PLA-based rigid films was followed by an investigation with an atomic force microscope. The changes in the molar mass of the PLA-based rigid films and (*R,S*)-PHB were evaluated by gel permeation chromatography, and the remaining material was characterised by electrospray mass spectrometry. The thermal properties and the changes in the crystallinity of the materials during degradation were characterised by differential scanning calorimetry and thermogravimetric analysis. Furthermore, the effects of the interaction between the polymer and the cosmetic ingredient (paraffin) monitored during the degradation experiment are reported.

Materials and methods

Materials

The plain poly[(*R,S*)-3-hydroxybutyrate] used in this study was synthesised at the Centre of Polymer and Carbon Materials in Zabrze by an original method for the laboratory scale synthesis of high-molar mass (*R,S*)-PHB. This method includes: (i) purification of the β-butyrolactone (β-BL) monomer through the oxidation of impurities and a drying process;[53] (ii) introduction of the metal-free initiator for anionic polymerisation (tetrabutylammonium acetate) to the spherical reactor with a heat exchanger containing the β-BL monomer at temperature of 4 °C; upon this introduction, the temperature of the reaction mixture is kept below 20 °C until the viscosity increases, and then the mixture is maintained at 30 °C; (iii) protonation (after 85 % monomer conversion, the reaction mixture is transferred to a reactor with an excess volume of $CHCl_3$ and an aqueous solution of HCl to protonate the growing chain end and to hydrolyse the unreacted monomer; then, the $CHCl_3$ solution of the polymer is concentrated on a rotary evaporator under reduced pressure and the obtained polymer is dried under vacuum at 40 °C). (*R,S*)-PHB (M_w = 100 000, M_w/M_n = 1.4) cannot be extruded as a film because of the amorphous properties of the polymer. PLA and PLA/(*R,S*)-PHB blends with 3 mol %, 9 mol %, 12 mol %, and 15 mol % of (*R,S*)-PHB (calculated from the NMR spectra from the methyl group of the components), PLA, 97PLA/3(*R,S*)-PHB, 91PLA/9(*R,S*)-PHB, 88PLA/12(*R,S*)-PHB and 85PLA/15(*R,S*)-PHB, respectively, were prepared as rigid films at the Institute for Engineering of Polymer Materials and Dyes (IMPIB Toruń, Poland) under the MARGEN project.[46] The poly(L-lactide) used in the blends was a commercial product from NatureWorks LLC, USA, type 2002D. The material characterisation has been previously described.[46]

The degradation simulant, liquid paraffin (99.98 %, water content: 0.016 % determined by the Karl Fischer method) from Pharmaceutical Laboratory COEL, Poland, was used without further purification.

Degradation experiment

The degradation experiment was conducted as described previously.[48,49] The stability test for cosmetic products requires the placement of samples under different environmental conditions for a specified period. These conditions are meant to simulate what will happen to the product during its lifecycle and should always correspond to the worst foreseeable conditions of contact between the plastic material and the product inside.[48] The high temperature testing is used as a predictor of long-term stability and was selected for the degradation experiment according to the ISO 15814: 1999 (E) standard. PLA-based rigid films with an average thickness of 300 μm and in strip sizes of 2 cm x 1 cm with an average mass of 0.11 g, compared to the (*R,S*)-PHB with an average mass of 0.07 g, were incubated at 70 °C (± 0.5 °C). Because (*R,S*)-PHB does not yield self-supporting films, crude (*R,S*)-PHB was used. In this case, only one side of the sample was exposed to degradation.[54]

Measurements

The morphologies of the PLA-based rigid film surfaces were investigated with an atomic force microscope (AFM). The AFM images were obtained in MultiMode with a NanoScope III D controller, Veeco, USA, equipped with a piezoelectric scanner with a scan range of 10 μm x 10 μm. Imaging of the samples was conducted in tapping mode, under ambient air conditions at a scan rate of 1 Hz using etched silicon probes (TESP, VEECO) with a nominal spring constant of 20–80 N m^{-1} and at a resonant frequency of 280–320 kHz.

The molar mass and molar-mass dispersity of the samples were determined by gel permeation chromatography (GPC) in $CHCl_3$ (GPC Solvent, stabilised with amylene, purity 99.8 %, Fischer Chemical) at 35 °C with an eluent flow rate of 1 mL min^{-1} and a set of two PLgel, 5 μm MIXED-C ultrahigh efficiency columns (Polymer Laboratories) with a mixed bed and a linear M_w range of 200–2000000. An isocratic pump (Spectra Physics 8800) was used as the solvent delivery system, and a differential refractive index detector (Shodex SE 61) stabilised to a temperature of 35 °C was applied. A 10 μL aliquot of 3 % w/v sample solution in $CHCl_3$ was injected. Polystyrene standards (Calibration Kit S-M-10, Polymer Laboratories) with narrow molar-mass dispersities were used to generate a universal calibration curve. The samples were measured using OmniSEC 4.1 (Viscotek) software.

Nuclear magnetic resonance ^1H (^1H NMR) spectra were recorded with a Bruker-Advance spectrometer operating at 600 MHz with Bruker TOPSPIN 2.0 software. $CDCl_3$ was used as the solvent, tetramethylsilane (TMS) was the internal standard, and spectra were recorded with 64 scans, a pulse width of 11 μs, and an acquisition time of 2.65 s.

The electrospray mass spectrometry (ESI-MS) analysis was performed on the low molar mass samples remaining after 52 weeks of degradation in paraffin. The analysis was performed with a Finnigan LCQ ion trap mass spectrometer (Finnigan, San Jose, CA). Samples of the remaining film were

dissolved in a water/methanol solution (1:1 v/v), and the solutions were introduced to the ESI source by continuous infusion with the instrument syringe pump at a rate of 10 μL min^{-1}. The LCQ ESI source was operated at 4.5 kV, and the capillary heater was set to 200 °C. Nitrogen was used as the nebulising gas. The analyses were performed in the positive- and negative-ion modes.

Differential scanning calorimetry (DSC) measurements were performed with a TA DSC 2010 apparatus (TA Instruments, New Castle, DE). The instrument was calibrated with high-purity indium and gallium. Three calorimetric traces were acquired for each sample at heating/cooling/heating rates of 10° min^{-1}. Samples with masses of approximately 4 mg were placed into crimped aluminium pans. The first calorimetric trace (I-scan, first heating run), in which the thermal history is suppressed, and the third calorimetric trace (III-scan, second heating run), were acquired from –50 °C to 200 °C, and the second calorimetric trace (II-scan, cooling run) was acquired from 200 °C to –50 °C. All of the experiments were performed under a nitrogen atmosphere (flow = 50 mL min^{-1}).

Thermogravimetric analysis (TGA) was performed with a TGA/DSC1 Mettler-Toledo thermal analyser at a heating rate of 10° min^{-1} in a stream of nitrogen (60 mL min^{-1}). The obtained TGA data were analysed with the Mettler-Toledo Star System SW 9.30.

Results and discussion

Our previous studies originally revealed that the PLA film degraded in a hydrophobic solvent, such as paraffin, because of the residual moisture content.[48,49] Thus, further research on more resistant (bio)degradable candidates for plastic cosmetic packages is underway in our laboratories. During degradation in paraffin, comprehensive material characterisation of the polylactide-based rigid films with poly[(*R,S*)-3-hydroxybutyrate] was performed and compared to plain poly[(*R,S*)-3-hydroxybutyrate] by AFM, GPC, NMR, ESI-MS, DSC and TGA. Monitoring the mass changes in the samples during the degradation process was unfortunately not possible because of difficulties in cleaning the viscous paraffin from the samples, especially after the disintegration of the samples.

Macroscopic evaluation

Macroscopic visual evaluation of the PLA-based rigid films during the degradation process showed erosion through the disintegration of the strips, which began in the 15th week of incubation for the PLA, 97PLA/3(*R,S*)-PHB and 91PLA/9(*R,S*)-PHB rigid films. Higher amounts of (*R,S*)-PHB results in an extension of the disintegration time to 26 weeks for the 88PLA/12(*R,S*)-PHB and 85PLA/15(*R,S*)-PHB rigid films (Fig. 1).

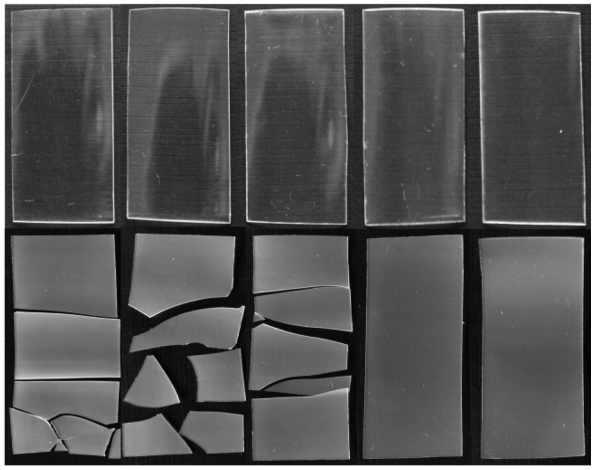

Fig. 1 – *Visual evaluation of the PLA, 97PLA/3(R,S)-PHB, 91PLA/9(R,S)-PHB, 88PLA/12(R,S)-PHB and 85PLA/15(R,S)-PHB rigid films correspondingly, before degradation (A) and after 15 weeks of degradation in paraffin (B)*

Before the degradation test, the PLA-based rigid films were transparent with a smooth surface. A decrease in the transparency of the studied sample surfaces (assumed to be caused by molecular reorganisation[55] or an increase in irregularity, which might result from the accelerated formation of new spherulites[56]) was observed for all the PLA-based rigid films from the beginning of the degradation process in paraffin. For a thicker rigid PLA film, this process is considerably faster than for the thin PLA film used in the previous degradation experiments.[48] Because thickness can affect the properties of the final product, this feature may be important from the perspective of the use of PLA-based rigid films in cosmetics packaging.

Molar mass changes

The degradation process in paraffin resulted in a continuous decrease in the molar mass of all the samples from the beginning of the experiment. As we observed in our previous studies, in an environment with residual moisture content, such as paraffin, degradation of the PLA film also occurred. The explanation for this unexpected phenomenon was the hydrophobicity of paraffin, which generated an autocatalytic effect in which the acid end-groups catalyse cleavage of the ester and the concentration of terminal chain ends with acid termination increases in the polymer.[32,47,49,57] Water initially diffused into the sample to penetrate the polymer matrix, and the process of autocatalytic hydrolysis began. The degradation process for a thicker rigid PLA film (thickness of 300 μm) is faster than for

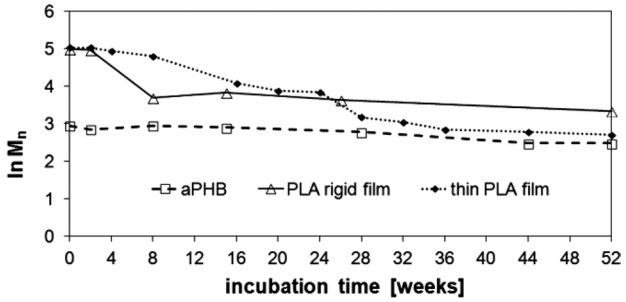

Fig. 2 – *Logarithmic number-average molar mass of the PLA rigid film (300 μm) and the thin PLA film (40 μm)[48] compared to (R,S)-PHB as a function of incubation time for the degradation process in paraffin over one year*

the thin PLA film (thickness of 40 μm) used in the previous degradation experiment.[48] Submillimetre films are known to degrade homogeneously and more slowly (erosion restricted at the surface) than devices with larger sizes.[58] The logarithmic M_n profiles of the PLA rigid film and the thin PLA film compared to (*R,S*)-PHB are presented in Fig. 2.

During the degradation of (*R,S*)-PHB, a molar mass decrease was observed from the beginning of the degradation experiment, although the decrease occurred more slowly. Poorly hydrophilic (*R,S*)-PHB degrades more slowly than hydrophilic PLA because the drying process is more difficult for amorphous regions of the polymer, the moisture is entrapped in the (*R,S*)-PHB polymer matrix and the hydrolysis process is accelerated from the beginning of the degradation experiment. The amount of moisture absorption depends on the crystallinity of the polymer. Amorphous forms of the polymer absorb moisture more rapidly than crystalline forms.[28,59]

The degradation rate of the PLA-based rigid films depended on the blend miscibility, as described above. The blends with poor miscibility (91PLA/9(*R,S*)-PHB, 88PLA/12(*R,S*)-PHB and 85PLA/15(*R,S*)-PHB rigid films) degraded comparable to the PLA rigid film and faster than the 97PLA/3(*R,S*)-PHB rigid film, which had good miscibility and a homogeneous surface morphology (see also Fig. 8). The results of gel permeation chromatography analysis showed shifts in the GPC traces to higher retention values for the molar mass: (*R,S*)-PHB > 97PLA/3(*R,S*)-PHB > PLA > 91PLA/9(*R,S*)-PHB > 88PLA/12(*R,S*)-PHB > 85PLA/15(*R,S*)-PHB rigid films, respectively (Fig. 3). In the first step, the addition of (*R,S*)-PHB reduces the degree of degradation in paraffin of the PLA-based rigid films only in the blend with good miscibility.

Because of the limited migration into the paraffin, the insoluble low-molar mass products remain in the degraded material (for all the PLA-based rigid films and (*R,S*)-PHB), and the molar mass dis-

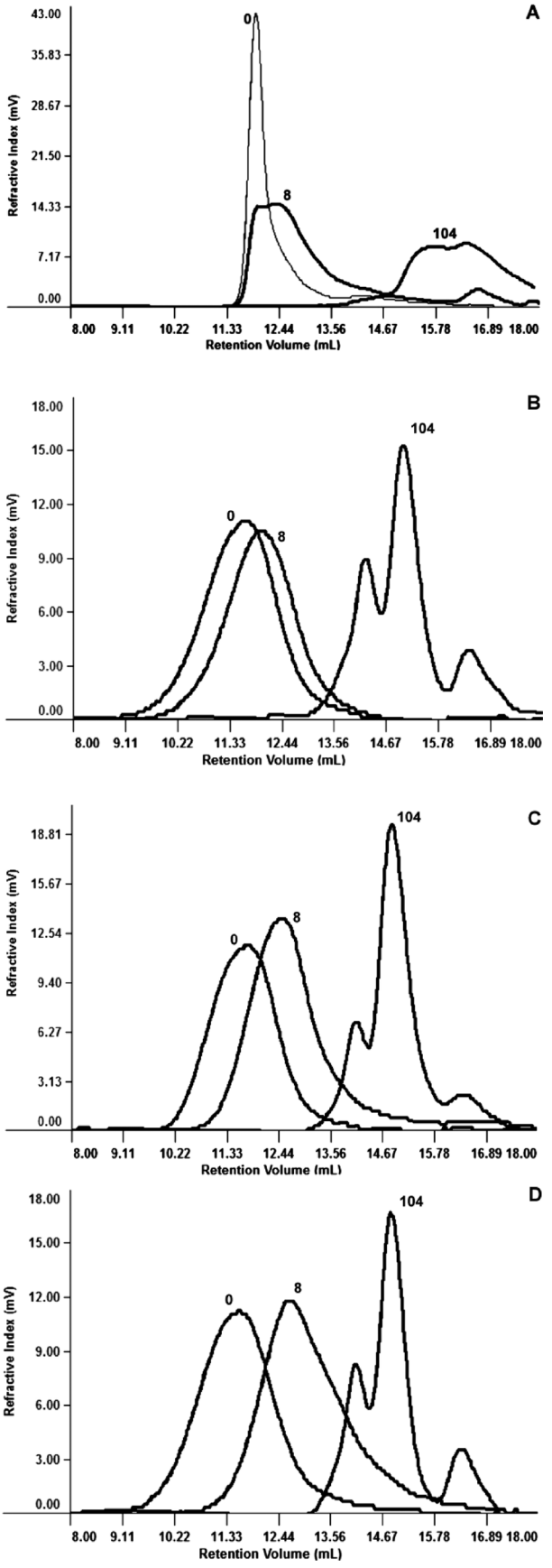

Fig. 3 – *Overlay of selected GPC chromatograms of (R,S)-PHB (A), 97PLA/3(R,S)-PHB (B), PLA (C), and 85PLA/15(R,S)-PHB (D) rigid films samples before degradation and after 8 and 104 weeks of degradation in paraffin*

persity increases rapidly between 8 and 28 weeks. Additionally, after 26 weeks of degradation in paraffin, multimodal GPC curves were observed for all the PLA-based rigid films (Fig. 3). We can explain the multimodal GPC chromatogram through two overlapping phenomena: (i) the result of the autocatalytic mechanism for different populations of macromolecules degrading at different rates at the surface/interior parts of the films[50,51] (the same effect was observed for PLA and 85PLA/15(*R,S*)-PHB rigid films) or (ii) the populations of the different oligomers for the two components of the blend.

Structural characterisation of the remaining material

The analysis by ^{1}H NMR (based on the methyl group of the components, data not shown) after predetermined degradation times indicated no significant changes in the compositions of all the blends investigated in the degradation experiment. The structure of the remaining (*R,S*)-PHB sample after 52 weeks of incubation in paraffin was determined by ESI-MS analysis.

Fig. 4 shows the positive ESI-mass spectrum acquired for the remaining (*R,S*)-PHB sample. Three series of singly charged ions of different intensities (one major and two minor) are observed in the mass spectrum and correspond to the three types of oligomer chains with a peak-to-peak mass increment of 86 Da, which is the molar mass of the 3-hydroxybutyrate repeating unit. The main series of signals, labelled (A), corresponds to the sodiated individual (*R,S*)-PHB oligomer chains terminated by hydroxy and carboxy end-groups. The second series of ions (with significantly lower relative intensity), labelled (B), can be assigned to the sodiated (*R,S*)-PHB oligomer chains terminated by crotonate and carboxy end-groups. The third series of ions, labelled (C), corresponds to the sodiated (*R,S*)-PHB oligomer chains terminated by acetate and carboxy end-groups. To verify the structural assignment of the ions presented in the ESI mass spectrum and to confirm the chemical structure of the remaining (*R,S*)-PHB sample, ESI-MS/MS experiments were performed for the ions at m/z of 901, m/z of 883 and m/z of 857 selected from the (A), (B) and (C) series, respectively.

Fig. 5 shows the ESI-MS/MS spectrum for the ion selected at m/z of 901, in series (A), which corresponds to the sodiated (*R,S*)-PHB oligomer with 10 repeating units (3-hydroxybutyrate units) terminated by hydroxy and carboxy end-groups. For this parent ion, fragmentation, which is caused by the random breaking of the ester bonds in the oligomer chains, leads to the formation of two series of product ions with a spacing of 18 Da. Based on the assigned structures, the product ions at m/z of 815, 729, 643, 557, 471 and 385 correspond to the (*R,S*)-PHB oligomers with hydroxy and carboxy end-groups. The complementary product ions at m/z of 797, 711, 625, 539, 453, 367 and 281 correspond to the (*R,S*)-PHB oligomer chains terminated by crotonate and carboxy end-groups. Thus, the product ion at m/z of 797 corresponds to the (*R,S*)-PHB

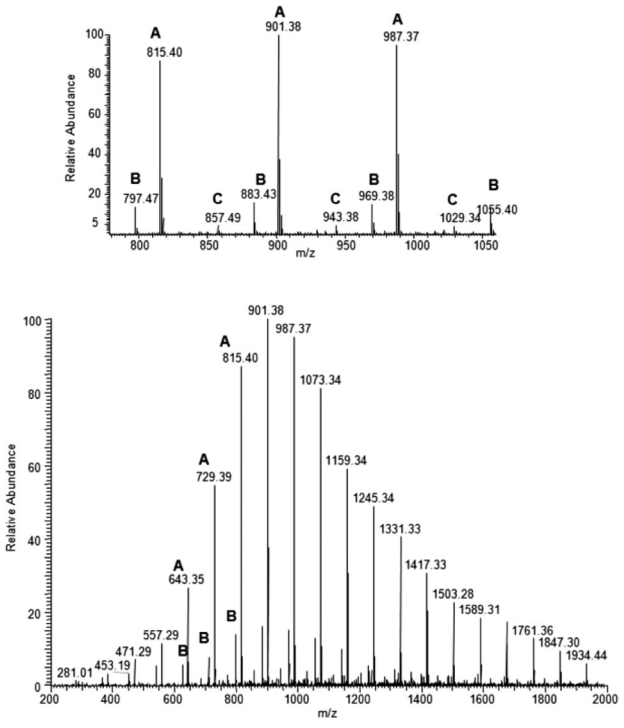

Fig. 4 – *ESI-mass spectrum (positive ion mode) of the remaining (R,S)-PHB sample after 52 weeks of incubation in paraffin, including the extended region from m/z of 780–1060*

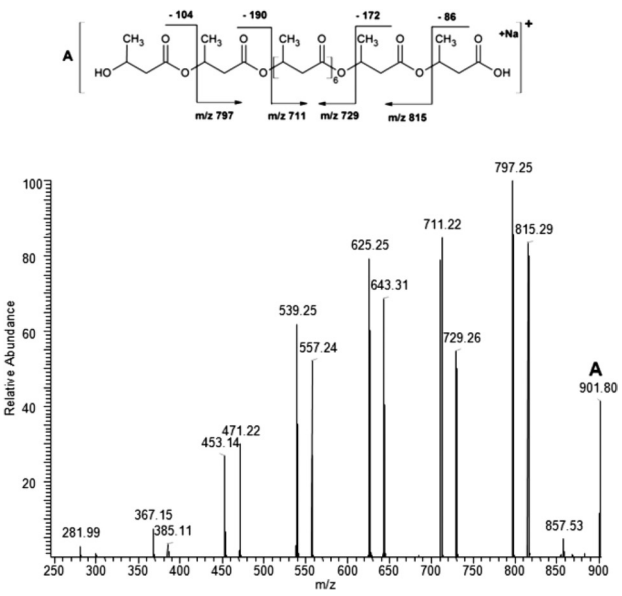

Fig. 5 – *ESI-MS/MS fragmentation experiments for the ion at m/z of 901 in series (A) (*Fig. 4*)*

oligomer formed by the loss of 3-hydroxybutyric acid (104 Da), and the product ion at m/z of 815 corresponds to the sodiated (*R,S*)-PHB oligomer formed by the loss of molecule of crotonic acid (86 Da).

Fig. 6 shows the results of the ESI-MS/MS experiment for the parent ion at m/z of 883 assigned to the sodiated (*R,S*)-PHB oligomer with a crotonate end-group. For this ion, fragmentation, which may occur from both sides of the molecule (see fragmentation pathway in Fig. 6), produces fragment ions exclusively through the loss of a neutral crotonic acid molecule.

Fig. 7 shows the results of the ESI-MS/MS experiment for the molecular ion at m/z of 857, which is assigned to the oligomer with an acetate end-group. The fragmentation of this ion also occurs along the oligomer chain (see fragmentation pathway in Fig. 7) through the formation of two sets of fragment ions with a spacing of 26 Da. Thus, the fragment ion at m/z of 797 corresponds to the oligomer ion formed by the loss of acetic acid (60 Da) from one side of the oligomer chain, and the ion at m/z of 771 corresponds to the oligomer ion formed by the expulsion of crotonic acid (86 Da) from other side of oligomer chain.

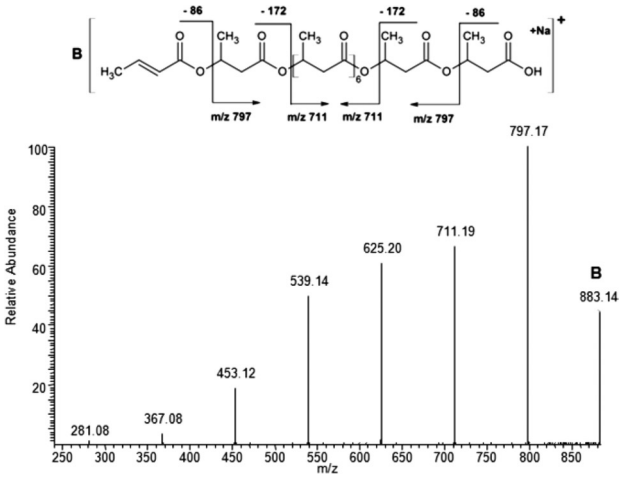

Fig. 6 – *ESI-MS/MS fragmentation experiments for the ion at m/z of 883 in series (B) (Fig. 4)*

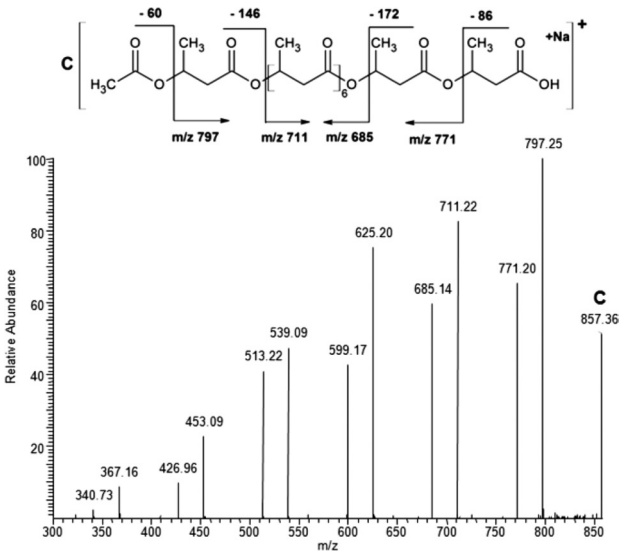

Fig. 7 – *ESI-MS/MS fragmentation experiments for the ion at m/z of 857 in series (C) (Fig. 4)*

The results of the ESI-MS^n analysis confirm that, after incubation in paraffin, the remaining (*R,S*)-PHB oligomers contain predominantly hydroxy and carboxy end-groups. The presence of hydroxy end-groups in the remaining (*R,S*)-PHB sample can result from the hydrolytic degradation of the initial high-molar mass (*R,S*)-PHB polyester caused by the water contained in the paraffin.[48] Additionally, small amounts of oligomers with crotonate and carboxy end-groups were observed. The formation of unsaturated (crotonate) end-groups in β-butyrolactone polymerisation was previously reported. These end-groups can be formed either in the initiation process or during propagation through a chain-transfer reaction to the monomer and through the recently reported E1cB intermolecular carboxylate-induced α-deprotonation mechanism of poly(3-hydroxyalkanoate)s.[60,61] Moreover, small amounts of oligomers with acetate end-groups have also been detected. The acetate end-groups were present in the original (*R,S*)-PHB sample with a high-molar mass and are derived from the initiator used during the preparation of this polymer sample.

Effect of miscibility on the degradation – surface morphology

The surface morphologies of the PLA-based rigid films before and after degradation in paraffin were characterised with an atomic force microscope. As described by Kikkawa *et al.*,[39,52] observation of the surface morphology by AFM can confirm the different miscibilities of the plain PLA-based rigid films. The blends with poor miscibility show phase-separation of the components (91PLA/9(*R,S*)-PHB, 88PLA/12(*R,S*)-PHB and 85PLA/15(*R,S*)-PHB rigid films, (Fig. 8) whereas a homogeneous surface morphology is observed for the blend with good miscibility (97PLA/3(*R,S*)-PHB rigid film, (Fig. 8). Additionally, the DSC curves for the 97PLA/3(*R,S*)-PHB rigid film showed a single glass transition temperature, indicating that the binary blend is miscible[62] (see Table 1). The diameter and depth of the pit domain increased as the (*R,S*)-PHB component increased in the blends, as observed by AFM. The plain PLA-based rigid films had surfaces with pit domains of up to 34 nm for the 85PLA/15(*R,S*)-PHB film. Only in the blend with good miscibility, the 97PLA/3(*R,S*)-PHB rigid film, is the surface completely smooth with a rough-

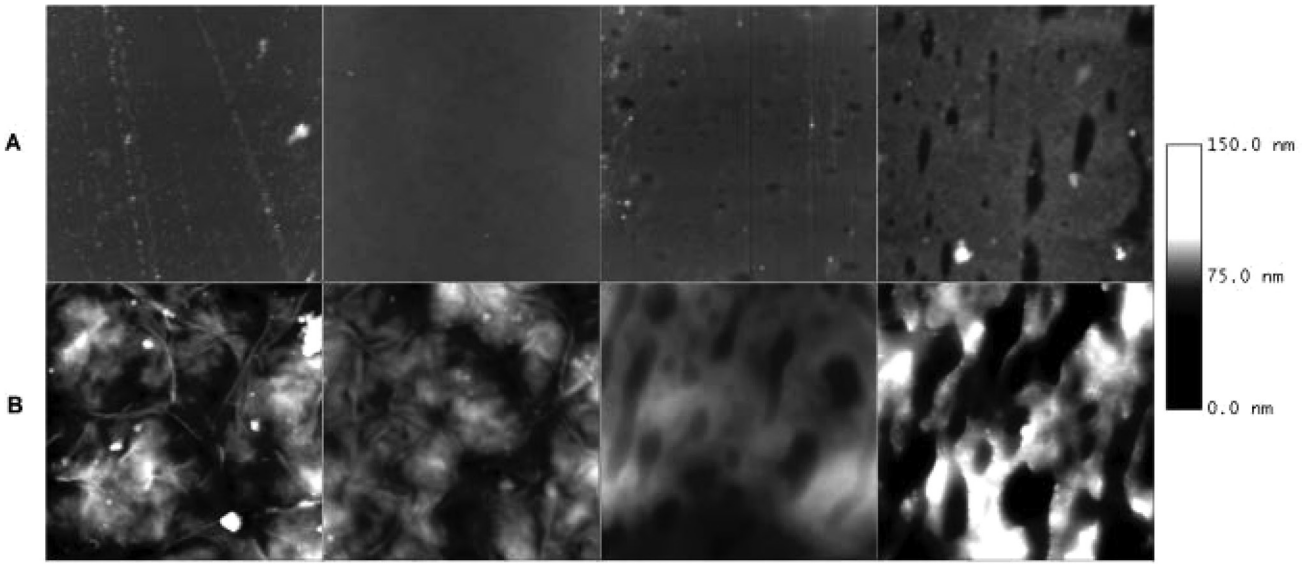

Fig. 8 – *Selected 6 x 6 μm AFM images of the surface erosion of PLA, 97PLA/3(R,S)-PHB, 91PLA/9(R,S)-PHB and 85PLA/15(R,S)-PHB rigid films, respectively, before (A) and after 52 weeks of the degradation process in paraffin (B)*

ness of 2 nm. During degradation, the surface becomes rougher for all the studied films; however, the difference in surface roughness was on the scale of nanometres (Fig. 8). In the AFM height image, dark and bright hues correspond to the low and high regions, respectively.

After 52 weeks of degradation, the pores of the rigid film surfaces had equal depths between 60 nm for the 97PLA/3(*R,S*)-PHB rigid film and 118 nm for the 85PLA/15(*R,S*)-PHB rigid film. The largest pores, observed after degradation, had an average depth of 118 nm, a length of 1.5 μm and a width of 1.1 μm, and were formed on the 85PLA/15(*R,S*)-PHB rigid film surface. The degree of erosion of the PLA-based rigid films was strongly dependent on the blend composition and the miscibility of the two components. The poor miscibility of the blend of 85PLA/15(*R,S*)-PHB rigid film with the largest pit domain before degradation, promoted roughness of the surface.

Thermal behaviour

The calorimetric parameters of the selected PLA-based rigid films during degradation were characterised by differential scanning calorimetry, and are given in Table 1.

The degradation rate of the PLA-based rigid films was assessed from the first heating run based on the work of Santonja-Blasco *et al.*[63] The cold crystallisation temperature (T_{cc}), the melting temperature (T_m) and the enthalpy values were obtained from the first calorimetric trace (first heating run) for the plain sample, and from the second heating run for the amorphous samples. The glass transition temperature (T_g) of the amorphous sample was obtained from the second calorimetric trace (cooling run), in which this transition temperature is the only phenomenon shown, because the applied cooling rate 10° min^{-1} does not allow for crystallisation. However, when the applied cooling rate allows crystallisation, amorphous samples were obtained by rapid cooling from the melt. The T_g was calculated to be the temperature at the inflection point of the phenomenon. Fig. 9 shows the DSC thermograms of the crude (*R,S*)-PHB, plain PLA and 85PLA/15(*R,S*)-PHB rigid films.

In the first calorimetric trace, the following transitions were observed along the increasing temperature-axis for the plain PLA rigid film: an endothermic phenomenon, the structural relaxation (observed at 65.6 °C) overlapped with the glass transition relaxation (between 50 °C and 70 °C), cold crystallisation (with a maximum at 128.9 °C)

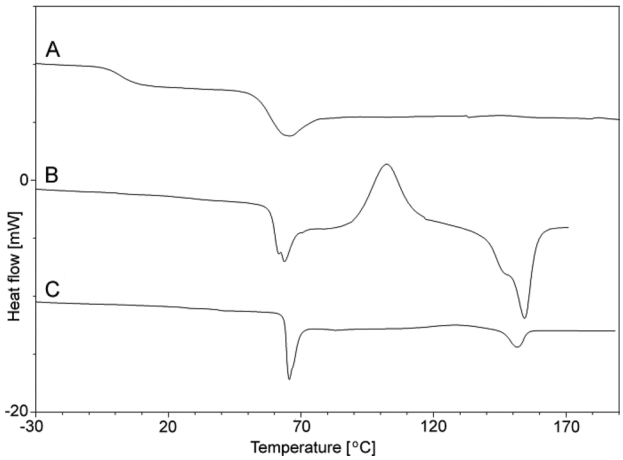

Fig. 9 – *DSC thermograms (first heating run) as a function of temperature for the plain crude (R,S)-PHB (A), 85PLA/15(R,S)-PHB (B) and PLA (C) rigid films*

Table 1 – *Calorimetric parameters during the degradation process of PLA and the selected PLA/(R,S)-PHB rigid films at 70 °C in paraffin (first heating run, 10° min^{-1})*

Incubation time [weeks]/sample	T_{g1} [°C]	T_{g2} [°C]	T_{cc} [°C]	ΔH_{cc} [J g^{-1}]	T_m [°C]	ΔH_m [J g^{-1}]
PLA						
0	–	57.0	128.9	3.5	151.6	3.7
15	–	46.7	–	–	147.8	43.1
26	–	42.8	–	–	146.9	45.2
52	–	42.2	–	–	139.6	53.8
104	–	40.4	–	–	143.7	61.5
97PLA/3(*R,S*)-PHB						
0	–	54.0	107.5	25.6	152.6	25.7
16	–	50.0	–	–	154.5	33.8
26	–	49.5	–	–	155.9	36.2
44	–	40.0	–	–	140.6	47.1
52	–	35.5	–	–	132.4	60.3
104	–	43.0	–	–	132.9	67.5
85PLA/15(*R,S*)-PHB						
0	–0.5	51.9	102.2	23.5	154.3	23.8
16	2.2	44.8	–	–	153.9	27.8
26	–	37.0	–	–	153.6	32.8
44	–	28.4	–	–	142.5	40.3
52	–	21.4	–	–	135.0	44.0
104	–	37.9	–	–	136.2	55.4
91PLA/9(*R,S*)-PHB						
0	1.4	57.0	106.0	26.2	151.5	26.9
88PLA/12(*R,S*)-PHB						
0	1.5	54.9	98.9	17.2	151.3	24.3

T_{g1} and T_{g2} – glass transition temperatures of the blend components determined for an amorphous sample, T_{cc} – maximum of the exothermic peak of the cold crystallisation temperature, ΔH_{cc} – cold crystallisation enthalpy, T_m – melting temperature, ΔH_m – melting enthalpy

and the melting process (with a maximum at 151.6 °C). The first heating run for all the PLA-based rigid films before incubation (Table 1) are similar, and show a glass transition overlapped with the structural relaxation followed by cold crystallisation and melting. The enthalpy values for the consecutive cold crystallisation and melting processes were the same, suggesting that all the plain PLA-based rigid films (except the slightly ordered 88PLA/12(*R,S*)-PHB blend) were amorphous before the degradation experiment, as evidenced by DSC. The presence of (*R,S*)-PHB can not only plasticise[64] but can also initiate the crystallisation of the blends by induction/nucleation as the nucleation agent[65] (ΔH_{cc} increases significantly, T_g decreases slightly, but T_{cc} significantly, Table 1). The induction/nucleation effect increased as the (*R,S*)-PHB content increased. For all the PLA/(*R,S*)-PHB rigid films, except the 97PLA/3(*R,S*)-PHB blend, two glass-transition temperatures were observed and indicated that the blends are immiscible and exhibit phase separation in the melt (Fig. 10). The T_g of a polymer in immiscible blends does not change with composition and is expected to maintain the value of the individual components, whereas in miscible blends, the glass transition temperatures of the components, shift toward each other.[39,66]

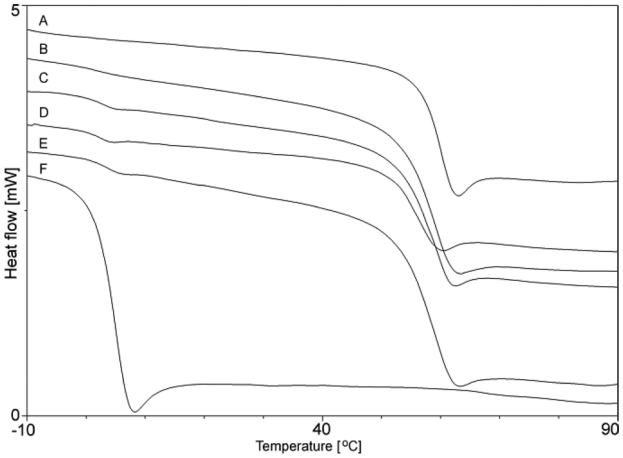

Fig. 10 – *DSC curves (second heating run) for the plain PLA (A), 97PLA/3(R,S)-PHB (B), 91PLA/9(R,S)-PHB (C), 88PLA/12(R,S)-PHB (D) and 85PLA/15(R,S)-PHB (E) rigid films as well as for crude (R,S)-PHB (F)*

During the second heating run at 10 °C min^{-1}, all the examined amorphous samples exhibited a cold crystallisation effect. Measurements were performed on the amorphous samples obtained after cooling at 10° min^{-1} (when the applied cooling rate of 10° min^{-1} does not allow crystallisation) or for amorphous samples obtained by quenching the melt with liquid nitrogen (rapid cooling, RC). The maximum of the exothermic peak of the cold crystallisation temperature decreased as the incubation time increased. Therefore, during the degradation process, the shorter chains could begin to freely crystallise at lower temperatures because of their higher mobilities. The degradation process increases the values of the cold crystallisation enthalpy. An increase in the cold crystallisation enthalpy indicates an increase in the number of polymer chains that are involved in the crystallisation process during degradation. The parameters evaluated in the analysis of the cold crystallisation are provided in Table 2.

Table 2 – *Calorimetric parameters related to the cold crystallisation and melting transitions for amorphous PLA and PLA/(R,S)-PHB rigid films during degradation at 70 °C in paraffin (second heating run, 10° min^{-1})*

Incubation time [weeks]/sample	T_{0n} [°C]	T_{cc} [°C]	ΔH_{cc} [J g^{-1}]	T_{m1} [°C]	T_{m2} [°C]
PLA					
0	110.0	129.6	3.4	–	151.7
15	90.0	99.4	40.62	135.5	149.6
26	90.0	99.3	40.5	–	147.4
52	80.0	89.5	47.5	–	143.9
104	94.0	115.0	26.0	–	142.5
97PLA/3(*R,S*)-PHB					
0	110.0	129.0	5.8	–	152.6
16	107.0	121.5	31.3	151.0	155.2
26	100.0	110.0	37.3	145.9	154.8
44	80.0	87.0	37.5	130.0	143.3
52	81.0	88.0	40.0	124.5	138.5
104	90.0	95.5	49.5	130.0	133.0
85PLA/15(*R,S*)-PHB					
0	110.0	129.0	6.1	–	152.9
16	96.0	110.0	31.0	145.9	154.8
26	90.0	98.0	30.4	140.4	153.4
44	76.0	82.0	33.2	129.0	143.3
52	67.0	74.4	34.4	–	136.7
104	90.0	96.0	44.0	127.7	132.7

T_{0n} – onset of the cold crystallisation temperature, T_{cc} – maximum of the exothermic peak of the cold crystallisation temperature, ΔH_{cc} – cold crystallisation enthalpy, T_{m1} and T_{m2} – melting temperatures of the crystalline conformations with smaller and larger sized lamella, respectively

During the second heating run of the PLA-based rigid films at 10° min^{-1}, the double melting endotherms were also observed after the cold crystallisation process. The lowest melting temperature peak corresponds to the population with a smaller size lamella, and the highest temperature peak corresponds to the crystalline conformations that have larger sized lamella. Multiple melting peaks in the DSC curves have been reported for many semicrystalline polymers. There is no single explanation for these peaks. In our case, the double melting peaks could result from the degradation mechanism, which can lead to the formation of dual populations of crystallites, as described by Wang *et al.*[49,67]

The influence of the degradation process in paraffin on the investigated samples was also characterised by thermogravimetric analysis. TG curves were obtained for the PLA, 97PLA/3(*R,S*)-PHB, and 85PLA/15(*R,S*)-PHB rigid films and for (*R,S*)-PHB during the degradation process at a heating rate of 10° min^{-1}. The degradation of the PLA rigid film and of (*R,S*)-PHB undergoes one stage of mass loss. After 52 weeks of degradation in paraffin, only one stage of mass loss was observed for the (*R,S*)-PHB. In contrast, for the 97PLA/3(*R,S*)-PHB and 85PLA/15(*R,S*)-PHB rigid films, two stages of mass loss were observed. For the PLA, 97PLA/3(*R,S*)-PHB and 85PLA/15(*R,S*)-PHB rigid films after degradation in paraffin, more complex mass losses were found (Fig. 11). The decomposition of PLA, 97PLA/3(*R,S*)-PHB and 85PLA/15(*R,S*)-PHB rigid films after degradation confirms the degradation mechanism, which can lead to the formation of dual populations of PLA crystallites,[49] as indicated by DSC. The first derivative (DTG) of the TG curve is a useful method to notice slight changes in the curves more easily. In Fig. 11, representative first-derivative TG curves are plotted for the (*R,S*)-PHB, PLA and 85PLA/15(*R,S*)-PHB rigid films during the degradation process. The averages of the total mass losses at 400 °C for all the investigated samples were approximately 100 %.

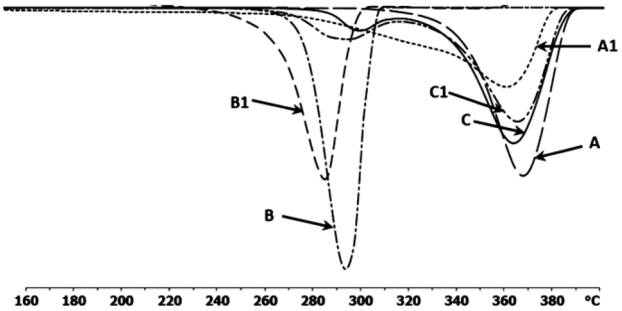

Fig. 11 – *Selected first-derivative TG curves before degradation of the PLA rigid film (A), the (R,S)-PHB (B) and the 85PLA/15(R,S)-PHB rigid film (C) and after 52 weeks of degradation in paraffin for the PLA rigid film, (R,S)-PHB, and the 85PLA/15(R,S)-PHB rigid film, A1, B1 and C1, respectively*

Conclusions

The current study constitutes an integrated approach to forensic engineering of advanced polymer materials with perspective application as compostable polymeric packing materials for products with a long shelf life. The degradation process in paraffin, the selected ingredient used as cosmetics simulant, for PLA-based rigid films was compared to (*R,S*)-PHB through a comprehensive material characterisation by AFM, GPC, NMR, ESI-MS, DSC and TGA techniques.

The degree of erosion of PLA-based rigid films was observed to be strongly dependent on the blend composition and the miscibility of the two components. The addition of (*R,S*)-PHB reduces the degree of degradation in paraffin during the first step

of degradation, as evidenced by GPC, for the PLA-based rigid films only in the blend with good miscibility, but higher amount of (*R,S*)-PHB results in an extension of the disintegration time in immiscible blends. Decreases in the glass transition and melting temperatures were observed during the degradation in paraffin for all the investigated materials. A decrease in the molar mass during the degradation process enabled the formation of crystalline structures among the short chains, and these structures increased the crystallinity of the material as the degradation time increased.

Degradation has a significant impact on the properties of the materials used for packaging applications, and this impact must be considered. As was originally observed[48,49], the degradation process in an environment with residual water content, such as paraffin, occurs and indicates morphological and structural transformations in investigated materials, but the addition of (*R,S*)-PHB reduces these processes. The (*R,S*)-PHB and PLA/(*R,S*)-PHB blends with good miscibility are (bio)degradable materials that are more resistant to degradation in cosmetic simulants; however, further studies on more suitable biodegradable candidates for plastic cosmetic packages are still needed.

ACKNOWLEDGEMENTS

This work was supported by the National Science Centre (NCN SONATA project no. 2012/05/D/ST5/03384, "Synthetic analogues of aliphatic biopolyesters generating controlled response in the form of a mechanical effect on temperature stimulus" and NCN OPUS project no. 2012/07/B/ST5/00627, "Low pressure catalytic synthesis of novel beta-lactone monomers and their anionic ring-opening (co)polymerisation leading to synthetic analogues of aliphatic biopolyesters"); the DoktoRIS project-scholarship program for innovation in Silesia supported by the European Community through the European Social Fund; the European Regional Development Fund, project MARGEN no. POIG.01.03.01–00–018/08, "New generation packaging materials made from plastics subject to organic recycling" in the framework of the Innovative Economy Operational Programme (IE OP) and by the European Commission under the Seventh Framework Programme (POLINNOVA project no. 316086). The outcomes of this research were used to implement the PLASTiCE project (3CE368P1, "Innovation value chain development for sustainable plastics in Central Europe", Central Europe Programme, co-financed by ERDF).

The authors would like to thank R. Malinowski of the IMPIB in Toruń, Poland, for the preparation of PLA-based rigid films.

References

1. *Lewis, P.R., Gagg, C.*, Forensic Polymer Engineering: Why polymer products fail in service, 1st ed., Woodhead Pub. Limited, Cambridge, 2010, pp 1–496. doi: http://dx.doi.org/10.1533/9781845697808.1
2. *Siracusa, V., Rocculi, P., Romani, S., Rosa, M.D.*, Biodegradable polymers for food packaging: a review, Food. Sci. Technol. **19** (2008) 634. doi: http://dx.doi.org/10.1016/j.tifs.2008.07.003
3. *Gross, R.A., Kalra, B.*, Biodegradable polymers for the environment, Science **297** (2002) 803. doi: http://dx.doi.org/10.1126/science.297.5582.803
4. *Magoń, A., Pyda, M.*, Study of crystalline and amorphous phases of biodegradable poly(lactic acid) by advanced thermal analysis, Polymer **50** (2009) 3967. doi: http://dx.doi.org/10.1016/j.polymer.2009.06.052
5. *Calafel, M.I., Remiro, P.M., Cortázar, M.M., Calahorra, M.E.*, Cold crystallization and multiple melting behavior of poly(L-lactide) in homogeneous and in multiphasic epoxy blends, Colloid. Polym. Sci. **288** (2010) 283. doi: http://dx.doi.org/10.1007/s00396-009-2156-3
6. *Torres, A., Li, S., Roussos, S., Vert, M.*, Poly(lactic acid) degradation in soil or under controlled conditions, J. Appl. Polym. Sci. **62** (1996) 2295. doi: http://dx.doi.org/10.1002/(SICI)1097-4628(19961226)62:13<2295::AID-APP14>3.0.CO;2-2
7. *Hakkarainen, M., Karlsson, S., Albertsson, A.C.*, Rapid (bio)degradation of polylactide by mixed culture of compost microorganisms – low molecular weight products and matrix changes, Polymer **41** (2000) 2331. doi: http://dx.doi.org/10.1016/S0032-3861(99)00393-6
8. *de Jong, S.J., Arias, E.R., Rijkers, D.T.S., van Nostrum, C.F., Kettenes-van den Bosch, J.J., Hennink, W.E.*, New insights into the hydrolytic degradation of poly(lactic acid): participation of the alcohol terminus, Polymer **42** (2001) 2795. doi: http://dx.doi.org/10.1016/S0032-3861(00)00646-7
9. *Rychter, P., Biczak, R., Herman, B., Smyłła, A., Kurcok, P., Adamus, G., Kowalczuk, M.*, Environmental degradation of polyester blends containing atactic poly(3-hydroxybutyrate). biodegradation in soil and ecotoxicological impact, Biomacromolecules **7** (2006) 3125. doi: http://dx.doi.org/10.1021/bm060708r
10. *Cairncross, R.A., Becker, J.G., Ramaswamy, S., O'Connor, R.*, Moisture sorption, transport and hydrolytic degradation in polylactide, Appl. Biochem. Biotech. **131** (2006) 774. doi: http://dx.doi.org/10.1385/ABAB:131:1:774
11. *Sikorska, W., Dacko, P., Sobota, M., Rydz, J., Musioł, M., Kowalczuk, M.*, Degradation study of polymers from renewable resources and their compositions in industrial composting pile, Macromol. Symp. **272** (2008) 132. doi: http://dx.doi.org/10.1002/masy.200851219
12. *Musioł, M.T., Rydz, J., Sikorska, W.J., Rychter, P.R., Kowalczuk, M.M.*, A preliminary study of the degradation of selected commercial packaging materials in compost and aqueous environments, Pol. J. Chem. Tech. **13** (2011) 55. doi: http://dx.doi.org/10.2478/v10026-011-0011-z
13. *Sikorska, W., Richert, J., Rydz, J., Musioł, M., Adamus, G., Janeczek, H., Kowalczuk, M.*, Degradability studies of poly(L-lactide) after multi-reprocessing experiments in extruder, Polym. Degrad. Stabil. **97** (2012) 1891. doi: http://dx.doi.org/10.1016/j.polymdegradstab.2012.03.049
14. *Capra, P., Briasco, B., Sorrenti, M., Catenacci, L., Sachet, M., Perugini, P.*, Preliminary evaluation of packaging-content interactions: Mechanical and physicochemical characterization of polylactide bottles, J. Appl. Polym. Sci. **131** (2014) 40067. doi: http://dx.doi.org/10.1002/app.40067

15. *Khosravi-Darani, K., Mokhtari, Z.B., Amai, T., Tanaka, K.*, Microbial production of poly (hydroxybutyrate) from C1 carbon sources, Appl. Microb. Biotechnol. **97** (2013) 1407. doi: http://dx.doi.org/10.1007/s00253-012-4649-0
16. *Khosravi-Darani, K., Vasheghani-Farahani, E., Tanaka, K.*, Hydrogen-oxidizing bacteria as poly(hydroxybutyrate) producers, Iran. J. Biotechnol. **4** (2006) 193. doi: http://dx.doi.org/10.5812/ijb
17. *Mokhtari-Hosseini, Z.B., Vasheghani-Farahani, E., Heidarzadeh-Vazifekhoran, A., Shojaosadati, S.A., Karimzadeh, R., Khosravi-Darani, K.*, Statistical media optimization for growth and PHB production from methanol by a methylotrophic bacterium, Bioresour. Technol. **100** (2009) 2436. doi: http://dx.doi.org/10.1016/j.biortech.2008.11.024
18. *Mokhtari-Hosseini, Z.B., Vasheghani-Farahani, E., Shojaosadati, S.A., Karimzadeh, R., Heidarzadeh-Vazifekhoran, A.*, Effect of feed composition on PHB production from methanol by HCDC of Methylobacterium extorquens (DSMZ 1340), J. Chem. Technol. Biotechnol. **84** (2009) 1136. doi: http://dx.doi.org/10.1002/jctb.2145
19. *Shah-Hosseini, Sh., Sadeghi, M.T., Khosravi-Darani, K.*, Simulation and model validation of batch phb production process using Ralstonia eutropha Iran. J. Chem. Chemical Eng. **22** (2003) 35.
20. *Khosravi-Darani, K., Vasheghani-Farahani, E., Shojaosadati, S.A.*, Application of the plackett-burman design for the optimization of poly(β-hydroxybutyrate) production by Ralstonia eutropha Iran. J. Biotechnol. **1** (2003) 155. doi: http://dx.doi.org/10.5812/ijb
21. *Khosravi-Darani, K., Vasheghani-Farahani, E., Shojaosadati, S.A.*, Application of the Taguchi Design for Production of Poly(β-hydroxybutyrate) by Ralstonia eutropha, Iran. J. Chem. Chemical Eng. **23** (2004) 131.
22. *Khosravi-Darani, K., Vasheghani-Farahani, E.*, Application of supercritical fluid extraction in biotechnology, Crit. Rev. Biotechnol. **25** (2005) 1. doi: http://dx.doi.org/10.1080/07388550500354841
23. *Khosravi-Darani, K., Vasheghani-Farahani, E., Yamini, Y.*, Solubility of poly(β-hydroxybutyrate) in supercritical carbon dioxide, J. Chem. Eng. Data **48** (2003) 860. doi: http://dx.doi.org/10.1021/je020168v
24. *Khosravi-Darani, K., Vasheghani-Farahani, E., Shojaosadati, S.A., Yamini Y.*, Effect of process variables on supercritical fluid disruption of Ralstonia eutropha cells for poly(R-hydroxybutyrate) recovery, Biotechnol. Prog. **20** (2004) 1757. doi: http://dx.doi.org/10.1021/bp0498037
25. *Focarete, M.L., Scandola, M., Dobrzyński, P., Kowalczuk, M.*, Miscibility and mechanical properties of blends of (l)-lactide copolymers with atactic poly(3-hydroxybutyrate) Macromolecules, **35** (2002) 8472. doi: http://dx.doi.org/10.1021/ma020940z
26. *Reichardt, R., Rieger, B.*, Poly(3-hydroxybutyrate) from carbon monoxide, Adv. Polym. Sci. **245** (2012) 49. doi: http://dx.doi.org/10.1007/12_2011_127
27. *Jedliński, Z., Kowalczuk, M., Kurcok, P., Adamus, G., Matuszowicz, A., Sikorska, W.*, Stereochemical control in the anionic polymerization of β-butyrolactone initiated with alkalimetal alkoxides, Macromolecules **29** (1996) 3773. doi: http://dx.doi.org/10.1021/ma951888s
28. *Freier, T., Kunze, C., Nischan, C., Kramer, S., Sternberg, K., Sa, M., Hopt, U.T., Schmitz K.P.*, In vitro and in vivo degradation studies for development of a biodegradable patch based on poly(3-hydroxybutyrate), Biomaterials **23** (2002) 2649. doi: http://dx.doi.org/10.1016/S0142-9612(01)00405-7
29. *Kurcok, P., Kowalczuk, M., Adamus, G., Jedliński, Z., Lenz, R.W.*, Degradability of poly(β-hydroxybutyrate)s. Correlation with chemical microstucture, JMS-Pure Appl. Chem. **A32** (1995) 875. doi: http://dx.doi.org/10.1080/10601329508010300
30. S*eebach, D., Brunner, A., Bachmann, B.M., Hoffmann, T., Kuhnle, F.N.M., Lengweiler, U.D.*, Biopolymers and oligomers of (R)-3-hydroxyalkanoic acids: contributions of synthetic organic chemists, Ernst Schering Research Foundation, Berlin, 1995, pp 1–105.
31. *Pawan, G.L.S., Semple, S.J.G.*, Effect of 3-hydroxybutyrate in obese subjects on very-lowenergy diets and during therapeutic starvation, Lancet **321** (1983) 15. doi: http://dx.doi.org/10.1016/S0140-6736(83)91560-X
32. *Siparsky, G.L., Voorhees, K.J., Miao, F.*, Hydrolysis of polylactic acid (PLA) and polycaprolactone (PCL) in aqueous acetonitrile solutions: autocatalysis, J. Polym. Environ. **6** (1998) 31. doi: http://dx.doi.org/10.1023/A:1022826528673
33. *Yu, G.E., Marchessault, R.H.*, Characterization of low molecular weight poly(β-hydroxybutyrate)s from alkaline and acid hydrolysis, Polymer **41** (2000) 1087. doi: http://dx.doi.org/10.1016/S0032-3861(99)00230-X
34. *Yu, J., Plackett, D., Chen, L.X.L.*, Kinetics and mechanism of the monomeric products from abiotic hydrolysis of poly[(R)-3-hydroxybutyrate] under acidic and alkaline conditions, Polym. Degrad. Stab. **89** (2005) 289. doi: http://dx.doi.org/10.1016/j.polymdegradstab.2004.12.026
35. *Rydz, J., Zawidlak-Węgrzyńska, B., Christova, D.*, Degradable Polymers, in Mishra M.K. (Ed.), Encyclopedia of Biomedical Polymers and Polymeric Biomaterials, CRC Press, New York, USA, 2015 (DOI: 10.1081/E-EBPP-120051258).
36. *Abe, H., Matsubara, I., Doi, Y.*, Physical properties and enzymic degradability of polymer blends of bacterial poly[(R)-3-hydroxybutyrate] and poly[(R,S)-3-hydroxybutyrate] stereoisomers, Macromolecules **28** (1995) 844. doi: http://dx.doi.org/10.1021/ma00108a007
37. *Focarete, M.L., Ceccorulli, G., Scandola, M., Kowalczuk, M.*, Further evidence of crystallinityinduced biodegradation of synthetic atactic poly(3-hydroxybutyrate) by PHB-depolymerase A from *Pseudomonas lemoignei*. blends of atactic poly(3-hydroxybutyrate) with crystalline polyesters, Macromolecules **31** (1998) 8485. doi: http://dx.doi.org/10.1021/ma981115e
38. *Ha, C.S., Cho, W.J.*, Miscibility, properties and biodegradability of microbial polyester containing blends, Prog. Polym. Sci. **27** (2002) 759. doi: http://dx.doi.org/10.1016/S0079-6700(01)00050-8
39. *Kikkawa, Y., Suzuki, T., Tsuge, T., Kanesato, M., Doi, Y., Abe, H.*, Phase, structure and enzymatic degradation of poly(L-lactide)/atactic poly(3-hydroxybutyrate) blends: an atomic force microscopy study, Biomacromolecules **7** (2006) 1921. doi: http://dx.doi.org/10.1021/bm0600163
40. *Kalnins, M., Øics, I., Savenkova, L., Viesturs, U.*, Environmentally degradable polymeric composite materials, British J. Sci. **1** (2011) 89.
41. *Arias, V., Höglund, A., Odelius, K., Albertsson, A.C.*, Tuning the degradation profiles of poly(L-lactide)-based materials through miscibility, Biomacromolecules **15** (2014) 391. doi: http://dx.doi.org/10.1021/bm401667b
42. *Koyama, N., Doi, Y.*, Miscibility of binary blends of poly[(R)-3-hydroxybutyric acid] and poly[(S)-lactic acid], Polymer **38** (1997) 1589. doi: http://dx.doi.org/10.1016/S0032-3861(96)00685-4

43. *Gazzano, M., Focarete, M.L., Riekel, C., Scandola, M.*, Structural study of poly(L-lactic acid) spherulites, Biomacromolecules **5** (2004) 53.
doi: http://dx.doi.org/10.1021/bm0343951
44. *Furukawa, T., Sato, H., Murakami, R., Zhang, J., Noda, I., Ochiai, S., Ozaki, Y.*, Comparison of miscibility and structure of poly(3-hydroxybutyrate-co-3-hydroxyhexanoate)/poly(l-lactic acid) blends with those of poly(3-hydroxybutyrate)/poly(l-lactic acid) blends studied by wide angle X-ray diffraction, differential scanning calorimetry, and FTIR microspectroscopy, Polymer **48** (2007) 1749.
doi: http://dx.doi.org/10.1016/j.polymer.2007.01.020
45. *Gerard, T., Budtova, T.*, Morphology and molten-state rheology of polylactide and polyhydroxyalkanoate blends, Eur. Polym. J. **48** (2012) 1110.
doi: http://dx.doi.org/10.1016/j.eurpolymj.2012.03.015
46. *Bartczak, Z., Galeski, A., Kowalczuk, M., Sobota, M., Malinowski, R.*, Tough blends of poly(lactide) and amorphous poly([R,S]-3-hydroxy butyrate) – morphology and properties, Eur. Polym. J. **49** (2013) 3630.
doi: http://dx.doi.org/10.1016/j.eurpolymj.2013.07.033
47. *Huda, M.S., Yasui, M., Mohri, N., Fujimura, T., Kimura, Y.*, Dynamic mechanical properties of solution-cast poly(L-lactide) films, Mater. Sci. Eng., **A333** (2002) 98.
doi: http://dx.doi.org/10.1016/S0921-5093(01)01834-2
48. *Rydz, J., Adamus, G., Wolna-Stypka, K., Marcinkowski, A., Misiurska-Marczak, M., Kowalczuk, M.M.*, Degradation of polylactide in paraffin and selected protic media, Polym. Degrad. Stab. **98** (2013) 316.
doi: http://dx.doi.org/10.1016/j.polymdegradstab.2012.09.010
49. *Rydz, J., Wolna-Stypka, K., Musioł, M., Szeluga, U., Janeczek, H., Kowalczuk, M.*, Further evidence of polylactide degradation in paraffin and in selected protic media. A thermal analysis of eroded polylactide films, Polym. Degrad. Stab. **98** (2013) 1450.
doi: http://dx.doi.org/10.1016/j.polymdegradstab.2013.05.005
50. *Li, S., Vert, M.*, Biodegradation of aliphatic polyesters, in Scott G. (Ed.), Degradable polymers. Principles and applications, 2nd ed., Kluwer Academic Publishers, Netherlands, 2002, pp 71–131.
doi: http://dx.doi.org/10.1007/978-94-017-1217-0_5
51. *Li, S.M., Garreau, H., Vert, M.*, Structure-property relationships in the case of the degradation of massive aliphatic poly-(α-hydroxy acids) in aqueous media, J. Mater. Sci.: Mater. Med. **1** (1990) 123.
doi: http://dx.doi.org/10.1007/BF00700871
52. *Kikkawa, Y., Suzuki, T., Kanesato, M., Doi, Y., Abe, H.*, Effect of phase structure on enzymatic degradation in poly(L-lactide)/atactic poly(3-hydroxybutyrate) blends with different miscibility, Biomacromolecules **10** (2009) 1013.
doi: http://dx.doi.org/10.1021/bm900117j
53. *Kowalczuk, M., Kurcok, P., Kawalec, M., Sobota, M., Michalak, M*. (Centre of Polymer and Carbon Materials Polish Academy of Sciences) Polish Pat. Appl. P-393751, 27 Jan 2011.
54. *Scandola, M., Focarete, M.L., Adamus, G., Sikorska, W., Baranowska, I., Świerczek, S., Gnatowski, M., Kowalczuk, M., Jedliński, Z.*, Polymer blends of natural poly(3-hydroxybutyrate-co-3-hydroxyvalerate) and a synthetic atactic poly(3-hydroxybutyrate). characterization and biodegradation studies, Macromolecules **30** (1997) 2568.
doi: http://dx.doi.org/10.1021/ma961431y
55. *Andersson, S.R., Hakkarainen, M., Inkinen, S., Södergård, A., Albertsson, A.C.*, Leads to higher hydrolytic stability but more acidic hydrolysis product pattern, Biomacromolecules **11** (2010) 1067.
doi: http://dx.doi.org/10.1021/bm100029t
56. *Cam, D., Suong-Hyu, H., Ikada, Y.*, Degradation of high molecular weight poly(L-lactide) in alkaline medium, Biomaterials **16** (1995) 833.
doi: http://dx.doi.org/10.1016/0142-9612(95)94144-A
57. *Wu, T.M., Hsu, S.F., Shih, Y.F., Liao, C.S.*, Thermal degradation kinetics of biodegradable poly(3-hydroxybutyrate)/layered double hydroxide nanocomposites, J. Polym. Sci. Part A: Polym. Chem. **46** (2008) 1207.
doi: http://dx.doi.org/10.1002/polb.21454
58. *Grizzi, I., Garreau, H., Li, S., Vert, M.*, Hydrolytic degradation of devices based on poly(DLlactic acid) size-dependence, Biomaterials **16** (1995) 305.
doi: http://dx.doi.org/10.1016/0142-9612(95)93258-F
59. Reliance Industries Limited. Marketing Technical Services 2003;
http://www.ril.com/downloads/pdf/drying.pdf (10.9.2013.).
60. *Adamus, G., Kowalczuk, M.*, Anionic ring-opening polymerization of β-alkoxymethylsubstituted β-lactones, Biomacromolecules **9** (2008) 696.
doi: http://dx.doi.org/10.1021/bm701077v
61. *Kawalec, M., Adamus, G., Kurcok, P., Kowalczuk, M., Foltran, I., Focarete, M., Scandola, M.*, Carboxylate-induced degradation of poly(3-hydroxybutyrate)s Biomacromolecules **8** (2007) 1053.
doi: http://dx.doi.org/10.1021/bm061155n
62. *Ohkoshi, I., Abe, H., Doi, Y.*, Miscibility and solid-state structures for blends of poly[(S)-lactide] with atactic poly[(R,S)-3-hydroxybutyrate, Polymer **41** (2000) 5985.
doi: http://dx.doi.org/10.1016/S0032-3861(99)00781-8
63. *Santonja-Blasco, L., Moriana, R., Badía, J.D., Ribes-Greus, A.*, Thermal analysis applied to the characterization of degradation in soil of polylactide: I. Calorimetric and viscoelastic analyses, Polym. Degrad. Stab. **95** (2010) 2185.
doi: http://dx.doi.org/10.1016/j.polymdegradstab.2010.08.005
64. *Malinowski, R., Żenkiewicz, M., Richert, S.*, Niektóre właściwości modyfikowanego polilaktydu, in Wróbel G. (Ed.), Polimery i kompozyty konstrukcyjne, Logos Press, Cieszyn, Gliwice, Poland, 2011, pp 299–305.
65. *Di Lorenzo, M.L., Sajkiewicz, P., Gradys, A., La Pietra, P.*, Optimization of melting conditions for the analysis of crystallization kinetics of poly(3-hydroxybutyrate), e-Polymers **27** (2009) 1.
66. *Thirtha, V., Lehman, R., Nosker, T.*, Glass transition effects in immiscible polymer blends. Proceedings of the Society of Plastics Engineers, ANTEC Conference, Boston, 2005, p 303–307.
doi: http://dx.doi.org/10.1063/1.2989086
67. *Wang, Y, Mano, J.F.*, Influence of melting conditions on the thermal behavior of poly(L-lactic acid), Eur. Polym. J. 41 (2005) 2335.
doi: http://dx.doi.org/10.1016/j.eurpolymj.2005.04.030